Veterinary Oncology

RESEARCH

Open Access

Gene expression profile comparison of primary and pulmonary metastatic lesions in a dog with appendicular osteosarcoma and hypertrophic osteopathy

Keita Kitagawa[1], Jessica Dryfhout[2], Alexander I. Engleberg[3], Ya-Ting Yang[3], Vilma Yuzbasiyan-Gurkan[3,4] and Paulo Vilar-Saavedra[1*]

Abstract

Hypertrophic osteopathy (HO) is a paraneoplastic syndrome, and the most notable cause in dogs is pulmonary metastatic osteosarcoma (OSA). Although many molecular factors in canine OSA have been shown in metastasis, little is known about the gene expression profile of HO secondary to metastatic OSA. Therefore, the purpose of this study was to compare the gene expression profiles between primary and metastatic OSA lesions from the same dog and to look for gene expression changes that can elucidate the molecular mechanism of metastases and HO. Tumoral samples were obtained from a 2-year-old, intact male, Labrador retriever. At the first visit, the patient presented with an appendicular OSA as the primary lesion. About 10 months later, the dog developed HO due to a single pulmonary metastasis. Using these primary and metastatic samples from the same dog, as well as normal canine osteoblasts, we investigated the gene expression profiling using the NanoString nCounter® Canine IO panel. A total of 180 differentially expressed genes were identified between malignant OSA cells and non-malignant canine osteoblasts. Furthermore, 5 genes (CCL17, VEGFC, C3, C4BPA, and FOS) were differentially expressed in comparison between primary and metastatic OSA samples. CCL17 and VEGFC were upregulated in the primary lesion compared to the metastatic lesion, while C3, C4BPA, and FOS were downregulated in the primary lesion relative to the metastatic lesion. Given that the metastatic lesion was relevant to the development of HO, the different gene expression profiles may be relevant to understanding the pathophysiology of HO.

Keywords Hypertrophic osteopathy, NanoString, Osteosarcoma, Paraneoplastic syndrome, Gene expression profile

*Correspondence:
Paulo Vilar-Saavedra
pvilarsaavedra@ufl.edu
[1] Department of Small Animal Clinical Science, College of Veterinary Medicine, University of Florida, 2089 SW 16 Ave, Gainesville, FL 32608, USA
[2] Veterinary Emergency Group, Anaheim, CA 92808, USA
[3] Department of Small Animal Clinical Sciences, College of Veterinary Medicine, Michigan State University, East Lansing, MI 48824, USA
[4] Department of Microbiology, Genetics and Immunology, College of Veterinary Medicine, Michigan State University, East Lansing, MI 48824, USA

Background

Canine hypertrophic osteopathy (HO) is a paraneoplastic syndrome associated with pulmonary tumoral lesions and is characterized by the symmetrical formation of periosteal new bone along the diaphysis of the long bones of the appendicular skeleton [1–4]. Clinical signs include lameness, lethargy, localized pain, and soft tissue swelling surrounding the affected bones [1–4]. The diagnosis of HO is made based on the clinical history, clinical signs, and radiographical changes [2–4]. Metastasectomy, a surgical intervention to remove one or more metastatic

lesions, can result in the control of HO by achieving the resolution of the clinical signs and the radiographical changes [2, 5, 6]. The pathogenesis of HO is not currently fully understood. The veterinary literature in this regard is null, and the scarce references in human literature propose two major hypotheses explaining the development of HO: neurological and humoral pathways [7–9]. Resolution of symptoms following vagotomy empirically suggests neurologic involvement in HO, whereas humoral pathway involvement is supported by increased release of serum growth factors, including growth hormone, growth hormone-releasing hormone, platelet-derived growth factor (PDGF), and vascular endothelial growth factor (VEGF) by the metastatic lesion [8–10].

Canine appendicular osteosarcoma (OSA) is the most common form of malignant bone cancer in dogs, which is locally aggressive and highly metastatic; OSA is also the most notable cause of paraneoplastic HO in dogs [2, 11]. Regarding the pathophysiology of canine OSA, many molecular and genetic factors have been investigated to explain the development of metastasis [12, 13]. The overexpression of delta Np63, a transcription factor belonging to p53 family, has been reported to be correlated with pulmonary metastases via increased secretion of VEGFA through activation of STAT3 [12]. In addition, the downregulation of STAT3 decreases the expression of VEGF, and conversely, activation of STAT3 increases VEGF expression, and may thus facilitate metastasis in OSA [13]. Also, in addition to STAT3 and delta Np63, TGF beta also regulates VEGF secretion. The inhibition of TGF beta1 decreases VEGF secretion, suggesting TGF beta1 is associated with angiogenesis via VEGF [14]. TGF beta signaling is suggested to promote distant metastasis by activating cell migration and neoangiogenesis in OSA [14]. Furthermore, the downregulation of CXCR4 by zoledronate treatment alters the pattern of metastasis in OSA, curtailing metastasis to the lungs, but, not to other organs, such as the nerves and skin, suggesting CXCR4 has some contribution to pulmonary metastasis in OSA [15].

Molecular investigations in metastasis in canine OSA until now have focused on the pathophysiology of the primary OSA lesion. Lately, however, proteomics for OSA has shown differences in protein expression between primary and metastatic lesions [16]. Identifying the differences in gene expression profiling between primary and metastatic lesions would provide us with critical information for further understanding the pathophysiology of HO, as well as the metastatic process in OSA. Hence, the purpose of this study was to compare the gene expression profiles between primary and metastatic OSA lesions from the same dog who developed HO due to metastatic OSA.

Materials and methods

Primary and metastatic osa samples

Primary and metastatic OSA samples were collected from a 2-year-old, intact male, Labrador retriever that presented to the Michigan State University (MSU) Veterinary Medical Center. Both appendicular and solitary pulmonary metastatic lesions were surgically removed, and histopathologic diagnoses were confirmed by board-certified pathologists at MSU.

Cell culture

Three normal osteoblast strains were used in the current study as controls. Among them, one canine osteoblast strain (CnOb) was purchased from Cell Application Inc. (San Diego, CA, USA). Additional two canine osteoblast cell strains were derived from two different healthy beagles in our lab as described [17]. All three CnOb cell strains were maintained with CnOb Growth Medium (Cell Application Inc., San Diego, CA, USA) and supplemented with 10% fetal bovine serum (Thermo Fisher Scientific, Waltham, MA, USA), antibiotics (0.1% gentamycin, Life Technologies, Carlsbad, CA, USA) and incubated in a humidified incubator at 37˚C with 5% CO_2. These three canine osteoblasts strains were shown to express common osteoblast markers, including osteocalcin and collagen type I alpha chain (COL1A1) via quantitative real-time PCR previously by our team [17].

RNA isolation

Formalin-fixed paraffin-embedded (FFPE) canine OSA tissues from primary and metastatic lesions were obtained from the MSU Veterinary Diagnostic Library. Total RNA was isolated from FFPE tissue blocks using the RNeasy FFPE Kit (Qiagen, Hilden, Germany) according to manufacturer's instructions. RNA was also isolated from canine osteoblasts using mirVana miRNA Isolation Kit with phenol (Thermo Fisher Scientific, Waltham, MA, USA). Each sample was processed in triplicate. Isolated RNA was immediately stored at -80˚C for further studies.

Data analysis by nanostring technology

Gene expression was evaluated using the NanoString nCounter® Canine IO (immuno-oncology) gene-expression panel comprising of 780 genes, developed using the CanFam3.1 reference genome. Targeted expression profiling was performed using isolated RNA from OSA samples and canine osteoblast cell lines. Differential gene expression analysis was performed comparing affected OSA samples to non-tumoral control osteoblast cells.

Further analysis compared expression levels between primary and metastatic OSA samples.

Statistical analysis

Data normalization, quality control, and functional and pathway analysis were performed by importing nCounter data onto the ROSALIND® analysis platform (https://www.rosalind.bio). Normalization, fold changes, and *p*-values were calculated in-platform following the nCounter® advanced analysis protocol comparing the geometric mean of housekeeping probes to sample counts from the same lane of the array. Housekeeping genes used for normalization were chosen based on the geNorm algorithm as used in the NormqPCR R library [18]. In addition to differential gene expression, gene set analysis (GSA) and cell type profiling were also performed using the ROSALIND platform [19]. Differential expression was determined as significant under the parameters of a fold-change > |1.5| and and an adjusted *P*-value < 0.05, using the Benjamini–Hochberg correction method. The ROSALIND platform performs enrichment analysis by referencing several database sources, such as Interpro, NCBI, MSigDB, REACTOME, and WikiPathways [20–25]. Volcano plots and heatmaps were generated on ROSALIND comparing OSA cells to osteoblast cells and primary OSA to metastatic OSA.

Results

Case history

A 2-year-old, intact male, Labrador retriever was presented for a progressive right hindlimb lameness of 2-months duration at MSU Veterinary Medical Center. The dog was non-weight bearing and moderate muscle atrophy of the right hindlimb was observed. There was a large firm mass of approximately 10 cm in diameter in the right proximal tibia, causing a decreased range of motion of the right stifle, and pitting edema distal to the stifle joint. For staging purposes, we obtained bloodwork, thoracic radiographs, pre- and post-contrast Computed tomography (CT) scan. Staging results did not reveal any remarkable abnormalities except for an irregular shaped, large mass associated with the caudal aspect of the proximal tibia by CT scan. The histopathology report of surgical biopsy sample obtained from the proximal tibia mass confirmed the diagnosis of chondroblastic OSA with a mitotic index of 77 in 10 high powered fields (Fig S1.). The dog then underwent a right hindlimb amputation; however, adjuvant chemotherapy was not pursued at that time per the owner's decision.

The dog was examined 314 days postoperatively because of lethargy and decreased appetite. The dog had progressive lameness, pyrexia of 40.4˚C, soft tissue swelling and pain in the extremities. Orthopedic examination revealed a decreased range of motion in both elbow and carpal joints and pain upon extension of elbows bilaterally. Blood work revealed inflammatory leukogram, mild-moderate elevated ALP [154 U/L (normal range: 10–92 U/L)], and low urea nitrogen [8 mg/dL (normal range: 12–27 mg/dL)], otherwise within reference intervals.

For the diagnostic imaging, thoracic radiographs revealed the presence of a large intrathoracic mass and a smoothly marginated periosteal proliferation along the right humerus. Also, in CT scan, periosteal proliferations were noted along the fore and remaining hindlimb including the right humerus, the left tibia, the left metatarsal bones, and the left femur. The CT scan further indicated a solitary mass in the cranial mediastinum or right cranial lung lobe. Fine needle aspiration of the mediastinal mass was done; the result of cytology report was consistent with OSA. Integrating these findings, the dog was diagnosed as HO secondary to pulmonary metastatic OSA. For the treatment of HO, the cranial mediastinal mass was surgically removed, and submitted for histopathology. The diagnosis of metastatic chondroblastic OSA was made based on the histopathology evaluation (Fig S2.). As adjuvant therapy following metastasectomy, carboplatin (250-300 mg/m^2 IV every 3 weeks) was given a total of 6 doses and without remarkable adverse effects throughout the chemotherapy.

Postoperative follow-up was done by physical examination with either radiographs or CT scan. Clinical improvement of HO was achieved 9 days after metastasectomy; the dog regained mobility without associated pain. The first postoperative CT scan, performed 58 days after metastasectomy, showed that the dog retained radiologic evidence of HO. The previously noted HO lesions persisted and most of them were slightly more severe in right thoracic limb involving the right scapula, right humerus, right metacarpal bones, and the bilateral radii, ulnae, and second metacarpal bones. Interestingly, the mild improvement of HO in the right scapula was found radiologically based on the CT scan at that time. No lameness nor pain on the legs were appreciated at the second postoperative CT scan (i.e., 128 days after metastasectomy). Palpation revealed no abnormal findings and the previously noted periosteal proliferation (i.e., HO lesion) confirmed no longer present in the right humerus by CT scan.

Gene expression profile analysis

We extracted RNA from FFPE samples and analyzed it with the NanoString nCounter® Canine IO panel, which has great sensitivity and specificity for elucidating the differentially expressed genes in OSA cells compared to non-tumoral osteoblasts [26, 27]. The extracted RNA was examined for its quality in the Tape station. The DV_{200}

(%) of metastatic samples ranged from 47.3 to 56.6%, resulting in an average of 52.4%, whereas the DV_{200} (%) from primary tumor samples ranged from 22.2 to 45.4%, resulting in an average of 30.7%. In the NanoString Quality Control (QC) parameters, we noted that all samples had an average of 90% representation of housekeeping genes, with none being under 80%. The NanoString assay requires at least 300 ng RNA per FFPE sample.

The overview of the gene expression data is presented in the heatmap in Fig. 1. Distinct expression profiles for both up- and downregulated genes across all samples can be appreciated in Fig. 1a. The volcano plot shows all samples plotted as a functional fold change vs. *p*-value (Figs. 1b and 2b). Genes that exhibited a significant ($p < 0.05$) and 1.5-fold change in expression compared to the control group were selected. Overall, 180 genes were differentially regulated; 121 of these were upregulated, whereas 59 were downregulated in OSA compared to control (Fig. 1b). Some of the top upregulated include genes involved in the immune response and cytokine production, such as SPP1, CXCL10, CXCR4, whereas other genes were associated with the cell signaling pathway, such as TNFRSF11A and KIT (Table S1). On the other hand, of the 59 downregulated genes, the most down-regulated genes included those involved in cell migration and the cell cycle, such as PTHLH, THBS1, CCND1, CCDN2, and CDKN1A among others (Table S2).

Of special interest to us were the differences in gene expression between the primary and metastatic lesions. Although the number of differential genes expressed was small, the heatmap showed distinct expression profiles for both up- and downregulated genes. (Fig. 2a). Overall, 5 genes were differently expressed. The CCL17 and VEGFC were significantly upregulated in primary lesion when compared to metastatic lesion, while FOS, C3, and C4BPA were significantly downregulated in primary lesion when compared to metastatic lesion (Fig. 2b). Fold changes of these differential gene expressions are summarized in Table 1.

Through ROSALIND®, several differentially expressed signaling pathways were identified. Pathway significance was determined by a Global Significance Score (GSS) rating based on gene set analysis (Table 2). The GSS measures the extent of the difference of overall differential gene expression between primary and metastasis OSAs within a distinct signaling pathway. GSSs are positive regardless of upregulation or downregulation,

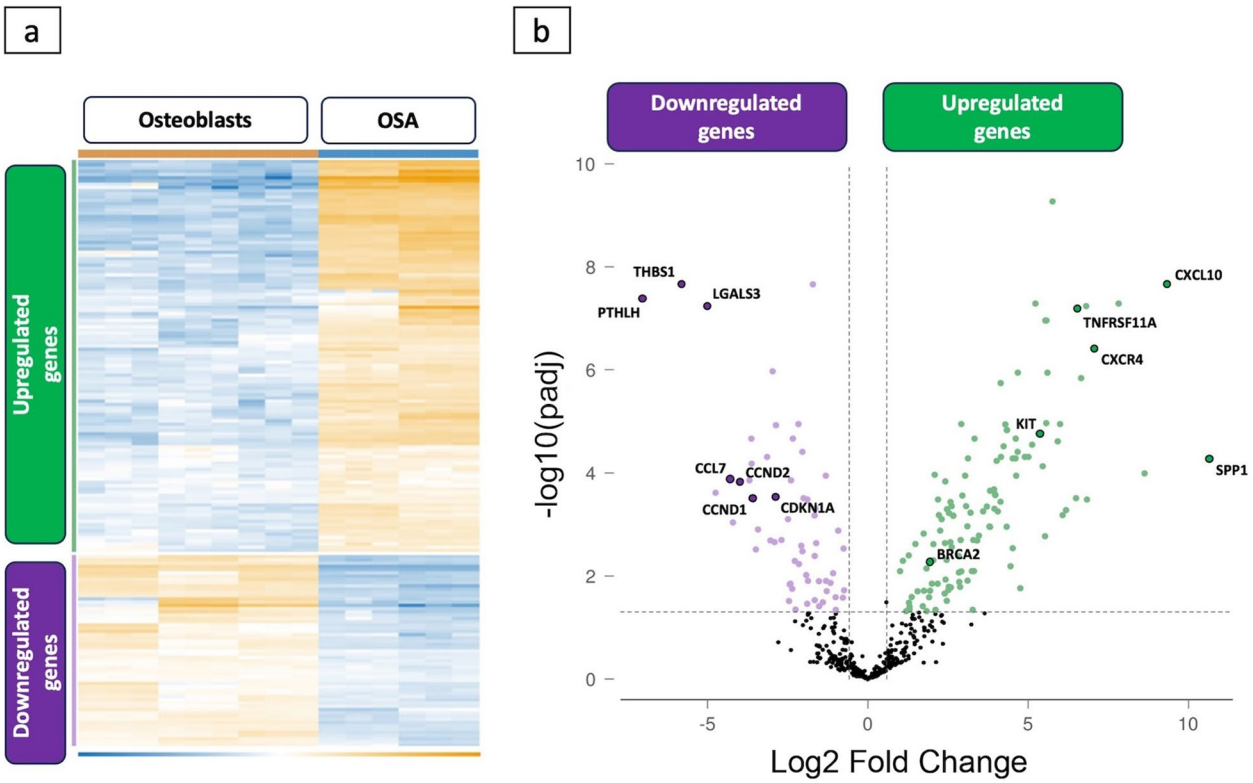

Fig. 1 Differential gene expression between primary and metastatic OSA and osteoblasts. **a** Heatmap of the gene expressions in canine osteoblast cells (in orange bar on top) and OSA cells (in blue bar on top). **b** Volcano plot of differential gene expressions in OSA cells relative to canine osteoblast cells. Green dots mean the gene upregulated and purple dots mean the gene downregulated

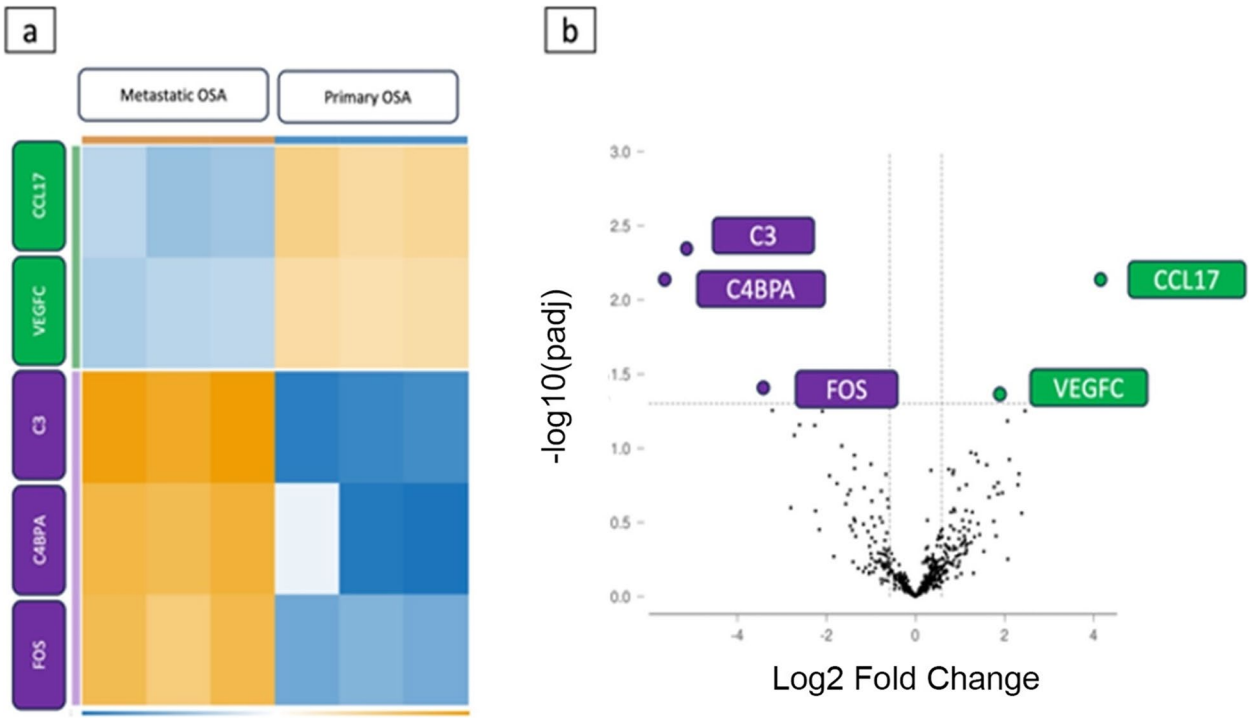

Fig. 2 Differential gene expression between primary and metastatic OSA. **a** The heatmap comparison of the gene expressions between metastatic OSA (in orange bar on top) and primary OSA (in blue bar on top)**. b** Volcano plot of differential gene expressions in primary OSA relative to metastatic OSA. Green dots indicate upregulated and purple dots indicate downregulated genes in primary OSA

Table 1 Genes with significant differential expression between the primary vs metastatic OS in this patient

Gene	Fold Change	Log_2 fold change
CCL17	+ 17.5	4.1
VEGFC	+ 3.7	1.9
FOS	- 11	-3.5
C3	- 34	-5.1
C4BPA	-48	-5.6

Table 2 Global significance ratings comparing overall differential expression of selected pathways between primary vs metastatic OSA

Term Name	Global Significance Score
Complement	1.6066
Complement System	1.415
NK Cell Functions	0.9216
Angiogenesis	0.8553
Chemokines	0.774
Wnt Signaling	0.7688
Interleukins	0.7613
Epigenetic Regulation	0.7612
Regulation	0.7441
TGF-beta Signaling	0.7385

with a large value indicating greater significance. The pathway with the highest GSS rating between primary and metastatic OSA was the Complement pathway with a score of 1.60. The other significant pathway was the Complement System pathway (1.41). The pathways with GSS ratings less than 1 included the NK cell functions pathway (0.92), the Angiogenesis pathway (0.85), the Chemokines pathway (0.77), the Wnt Signaling pathway (0.77), the Interleukins pathway (0.76), the Epigenetic Regulation pathway (0.76), the Regulation pathway (0.74) and the TGF-beta signaling pathway (0.74). The detailed information of these pathways was summarized in the Table S3.

Discussion

The clinical history of our OSA-HO case, including blood work results, radiographic findings, and the radiological resolution of HO after metastasectomy, are consistent with the previous studies [2–5]. Therefore, it is an archetypical subject of analysis for further understanding the pathophysiology of HO and OSA in dogs. When

comparing the gene expression profile of OSA vs. control, 180 genes were identified show significant differential expression. The most upregulated gene was SPP1 (Secreted Phosphoprotein 1), the protein-coding gene for Osteopontin (OPN), a structural protein of bone with extracellular matrix binding and cytokine activities. OPN exerts a regulatory effect in the differentiation of osteoblasts and enhances the metastatic potential of OSA tumoral cells at high levels by activating metalloproteinases [28]. OPN also promotes oncogenesis and metastasis by inhibiting apoptosis and stimulating the endurance of tumoral cells and neovascularization [29–31]. OPN modulates the immune system and possesses multiple roles in the inflammatory process [29, 32]. It serves as a chemotactic molecule to promote the migration of inflammatory cells and regulates dendritic cell responses [29, 33]. OPN is currently being studied as a potential cancer biomarker and target for the treatment of cancer [28]. CXCL10 encodes for a pro-inflammatory cytokine that binds to the CXCR3 receptor predominantly expressed on immune cells (e.g., lymphocytes, macrophages, dendritic cells). This protein binding results in pleiotropic effects, including alterations of the tumor microenvironment and cytokine storms, as documented in SARS Co V-2 infections [34, 35]. The overexpression of CXCL10 has been associated with both antitumoral attributes and disease severity (hematologic and solid) depending on the type of cancer [36, 37]. CXCR4 oncogene encodes a chemokine receptor, which activation transduces a signal resulting in modulation of the AKT signaling cascade and MAPK1/MAPK3 activation. High expression of CXCR4 correlated with the evidence of pulmonary metastasis in human OSA; additionally, the CXCR4 ligand, CXCL12, promotes metastasis, angiogenesis, and growth of OSA cells [38–40]. Fan et al. has shown that the inhibition of CXCR4 by zoledronate alters the metastatic behavior in canine OSA [15]. Some of the activities of the proteins encoded by the genes mentioned above (i.e., SPP1, CXCL10, CXCR4) could enable or partially explain some of the clinical findings (i.e., pulmonary metastasis) observed in our case.

The most downregulated gene was PTHLH, which encodes a protein involved in the regulation of endochondral bone development, as well as epithelial-mesenchymal interactions during the formation of mammary glands and teeth [41–43]. The overexpression of its receptor PTHR1 in OSA has been associated with increased invasion and proliferation and conversely, decreased mRNA expression of PTHR1 has been associated with inhibition of proliferation, migration, and invasion in human OSA cell lines [44, 45]. Patients with strong staining for PTHR1 in canine OSA tumors had reduced survival times compared to those with weak immunostaining intensity [45]. Another downregulated gene was THBS1, a gene that encodes for the TSP1 protein, a glycoprotein that mediates cell-to-cell and cell-to-matrix interactions. This protein promotes cell migration and metastasis via FAK pathway and is highly upregulated in lung metastatic OSA [46]. Similar associations with tumorigenesis, metastasis, and endothelial to mesenchymal transition have been described for the overexpression of LGALS3 protein and monocyte chemotactic protein 3(also known as CCL7) that encodes and is widely expressed in multiple cell types [47, 48]. We suspect that the downregulation of those genes (i.e., PTHLH, THSB1, LGALS3, CCL7) could be a cause or an effect on the OSA & HO pathogenesis. For example, Mainetti et al., showed that the KIT upregulation and activation stimulated cell migration by suppressing BRCA2 in human prostate carcinoma cells [49]. In our case, we observed the upregulation of KIT but not the downregulation of BRCA2. The KIT – BRCA2 regulatory interaction serves as an example of the complexity of cellular pathway interactions that could explain differences in gene expression profiles noted above.

When comparing the gene expression profile between primary and metastatic OSA lesions, we found the upregulation of CCL17 and VEGFC in primary lesion compared to metastasis. CCL17 and VEGFC proteins function as a cytokine and growth factor, respectively [50, 51]. Regarding the upregulation of CCL17 in the primary lesion, mature regulatory dendritic cells (mreg DCs) are tumor-specific and express CCL17 in human OSA [52]. Liu et al. showed mreg DCs were enriched in OSA but absent in PBMCs, suggesting that mreg DCs are tumor-associated and may be immunosuppressive in the tumor microenvironment [52]. Hence, the upregulation of CCL17 in the primary OSA may reflect a similar tumor microenvironment to human OSA, where it has enriched mreg DCs expressing CCL17.

Regarding the VEGFC upregulation found in the primary lesion, the study by Park et al. demonstrated that OSA cell lines expressed 2–fivefold higher amplification of VEGFC mRNA than the control, and the higher VEGFC expression was associated with high-grade histologic type. [53] In addition, a study by Yang et al. found that a higher VEGFC expression correlated with a higher tumor grade in chondrosarcoma [54]. Canine OSA is generally deemed a high-grade tumor, and the presence of a high mitotic index (77 in 10 high-powered fields) in our case is concordant with those findings.

FOS, C3, and C4BPA genes had significantly lower expression in primary lesion relative to metastasis. FOS is a proto-oncogene in humans; the overexpression of endogenous c-fos results in the development of OSA in transgenic mice [55]. Also, C4BPA is a protein-coding gene that promotes cancer cell proliferation in

CD40-expressing pancreas cancer [56]. Liu et al. reported that C4BPA and FOS were significantly upregulated in metastatic human OSA compared to non-metastatic OSA [57]. Similar to the findings of Liu et al., in our data, downregulation of FOS and C4BPA in primary lesion was found compared to metastasis. Thus, the upregulation of FOS and C4BPA could be a gene expression profile associated with metastatic lesions in canine OSA.

The comparison of GSA between primary and metastatic lesions revealed that the upregulation of C4BPA and C3 genes in the metastatic lesions mainly contributed to the predominance of the Complement and Complement System. C4BPA is an isoform of acute phase protein C4BP, and during inflammation, circulating C4BP levels may increase up to 400% mainly driven by the increase in isoform C4BPA level [58, 59]. C3 is also associated with inflammatory responses; it was upregulated at mRNA level in human endometriosis cells compared to non-inflammatory healthy control [60]. In addition, patients with HO had elevated complement levels, including C3 and C4 [61]. Hence, activating the complement pathways through the upregulation of C3 and C4BPA may explain the inflammatory process observed in HO, such as pyrexia or pain in the extremities.

Regarding quality assurance and control, we utilized DV_{200}, a metric representing the percentage of RNA fragments greater than 200 nucleotides after DNA extraction. This tool accurately evaluates RNA quality [62]. Given that RNA extracted from FFPE samples can be degraded due to formalin fixation methods and the age of archival samples, assessing RNA quality is crucial for ensuring reliable results [63]. According to Fujii et al., their DV_{200} ranged from 7.3% to 81%, with values below 30% deemed unsuitable for NGS library synthesis [64]. In our study, the average DV_{200} for primary and metastatic samples was 30.7% and 52.4%, respectively, indicating that the quality of RNA extracted from each sample was acceptable.

This study had some limitations. First, our sample size was small due to the nature of case reports. Second, due to the limitation of technical inheritance, differentiating the gene expressions derived from tumor cells from those from the tumor microenvironment was not possible because we employed a bulk analysis but not a spatial gene expression analysis. Lastly, investigating the interaction between the tumor microenvironment and its location was challenging due to the complexity of HO. In our case, given that metastasectomy resolved this case's HO, the cause and effect were clear. Thus, it seemed reasonable to compare gene expression profiles between primary and metastatic lesions.

Lung lesions, including but not limited to lung metastasis (e.g., Dirofilariasis), can cause HO [1, 2]. However, not all individuals with lung lesions develop HO. To address this, further comparative studies are needed: (a) between metastatic osteosarcoma (OSA) and adjacent, presumptive normal lung tissue, and (b) between dogs with lung lesions that do and do not develop HO. There is a possibility that a primary tumor might express HO-related genes that trigger HO when lung metastasis occurs. Future research should aim to identify any genes that are highly expressed in primary tumors and/or metastatic sites compared to osteoblast controls.

In summary, the five differentially expressed genes identified here provide clues for unraveling the pathophysiology of HO and pulmonary metastasis in canine OSA. Specifically, we found the upregulation of CCL17, VEGFC, and the downregulation of FOS, C3, and C4BPA in the primary lesion compared to the metastatic lesion in the same dog with HO caused by solitary metastasis of OSA. Further studies with more cases are needed to systematically explore the significance of these changes and explore gene expression more extensively in HO cases. The IO panel consists of 780 genes most of which are involved in tumorigenesis and as well as some genes reflecting immune pathways and immune cells and is thus not as comprehensive a look into the transcriptome as bulk RNA sequencing. However, it has great sensitivity and specificity, even when formalin fixed, and paraffin embedded samples are used and is therefore very useful for analysis of clinical samples. Our data presented here may form the basis of further comparisons if additional cases are acquired.

Abbreviations

CnOb	Canine osteoblast
COL1A1	Collagen type I alpha chain
CT	Computed tomography
FFPE	Formalin-fixed paraffin-embedded
GSS	Global Significance Score
HO	Hypertrophic osteopathy
MSU	Michigan State University
OPN	Osteopontin
OSA	Osteosarcoma
PDGF	Platelet-derived growth factor
SPP1	Secreted Phosphoprotein 1
VEGF	Vascular endothelial growth factor

Supplementary Information

The online version contains supplementary material available at https://doi.org/10.1186/s44356-024-00006-z.

Supplementary Material 1.

Acknowledgements

The authors thank the Genomics Core of the Research and Technology Support Facility of Michigan State University for the NanoString assay. The authors also want to thank Dr. Sarah Corner, Danielle Woodbury, Theresa Cyr and Krista Simmer for their extremely valuable support.

Authors' contributions

P.V.S. and V.Y.G conceived the original idea and design. K.K., J.D., and P.V.S. were involved in clinical data acquisitions and interpretations. K.K., A.I.E., Y.-T. Y, P.V.S, and V.Y.-G. were involved in the production, acquisition, and interpretation

of transcriptomic data. K.K., J. D, Y.-T. Y, A.I.E., V.Y.-G., and P.V.S. were involved in writing, reviewing, and editing the manuscript. P.V.S. and V.Y.-G. contributed to the final critical revision of the manuscript on their experience on the topic. All authors read and approved the final manuscript.

Funding
The authors received no external financial support for the research, authorship, and/or publication of this article.

Availability of data and materials
Data is available from the authors upon reasonable request and with permission of NanoString.

Declarations

Ethics approval and consent to participate
This study followed the guidelines approved by the VTH -MSU Ethics Committee. The dog in this study was examined and treated with the owner's written consent.

Consent for publication
The owner signed an informed consent form including the authorization to publish the data arising from this study.

Competing interests
The authors declare no competing interests.

Received: 17 May 2024 Accepted: 3 September 2024
Published online: 04 October 2024

References

1. Brodey RS. Hypertrophic osteoarthropathy in the dog: a clinicopathologic survey of 60 cases. J Am Vet Med Assoc. 1971;159(10):1242–56.
2. Withers SS, Johnson EG, Culp WT, Rodriguez CO Jr, Skorupski KA, Rebhun RB. Paraneoplastic hypertrophic osteopathy in 30 dogs. Vet Comp Oncol. 2015;13(3):157–65.
3. Pachamé AV, Beltrán MJ, Recchiuti NE, Portiansky EL, Massone AR, Gimeno EJ. Lesions of hypertrophic osteopathy in the forelimbs of a dog associated with pulmonary metastasis from a periosteal osteosarcoma. BJVP. 2017;10(2):61–4.
4. Ramoo S. Hypertrophic osteopathy associated with two pulmonary tumours and myocardial metastases in a dog: a case report. N Z Vet J. 2013;61(1):45–8.
5. Liptak JM, Monnet E, Dernell WS, Withrow SJ. Pulmonary metastatectomy in the management of four dogs with hypertrophic osteopathy. Vet Comp Oncol. 2004;2(1):1–12.
6. Turner H, Séguin B, Worley DR, Ehrhart NP, Lafferty MH, Withrow SJ, et al. Prognosis for dogs with stage III osteosarcoma following treatment with amputation and chemotherapy with and without metastasectomy. J Am Vet Med Assoc. 2017;251(11):1293–305.
7. Treasure T. Hypertrophic pulmonary osteoarthropathy and the vagus nerve: an historical note. J R Soc Med. 2006;99(8):388–90.
8. Nomori H, Kobayashi R, Kubo A, Morinaga S, Shintani Y, Sano T. Lung cancer containing growth hormone-releasing hormone associated with hypertrophic osteoarthropathy. Scand J Thorac Cardiovasc Surg. 1994;28(3–4):149–52.
9. Mito K, Maruyama R, Uenishi Y, Arita K, Kawano H, Kashima K, et al. Hypertrophic pulmonary osteoarthropathy associated with non-small cell lung cancer demonstrated growth hormone-releasing hormone by immunohistochemical analysis. Intern Med. 2001;40(6):532–5.
10. Ooi A, Saad RA, Moorjani N, Amer KM. Effective symptomatic relief of hypertrophic pulmonary osteoarthropathy by video-assisted thoracic surgery truncal vagotomy. Ann Thorac Surg. 2007;83(2):684–5.
11. Fenger JM, London CA, Kisseberth WC. Canine osteosarcoma: a naturally occurring disease to inform pediatric oncology. ILAR J. 2014;55(1):69–85.
12. Cam M, Gardner HL, Roberts RD, Fenger JM, Guttridge DC, London CA, et al. ΔNp63 mediates cellular survival and metastasis in canine osteosarcoma. Oncotarget. 2016;7(30):48533–46.
13. Fossey SL, Liao AT, McCleese JK, Bear MD, Lin J, Li PK, et al. Characterization of STAT3 activation and expression in canine and human osteosarcoma. BMC Cancer. 2009;9:81.
14. Portela RF, Fadl-Alla BA, Pondenis HC, Byrum ML, Garrett LD, Wycislo KL, et al. Pro-tumorigenic effects of transforming growth factor beta 1 in canine osteosarcoma. J Vet Intern Med. 2014;28(3):894–904.
15. Byrum ML, Pondenis HC, Fredrickson RL, Wycislo KL, Fan TM. Downregulation of CXCR4 expression and functionality after zoledronate exposure in canine osteosarcoma. J Vet Intern Med. 2016;30(4):1187–96.
16. Roy J, Wycislo KL, Pondenis H, Fan TM, Das A. Comparative proteomic investigation of metastatic and non-metastatic osteosarcoma cells of human and canine origin. PLoS One. 2017;12(9):e0183930.
17. Yang Y-T, Engleberg AI, Yuzbasiyan-Gurkan V. Establishment and characterization of cell lines from canine metastatic osteosarcoma. Cells. 2024;13(1):25.
18. Danaher P, Warren S, Dennis L, D'Amico L, White A, Disis ML, et al. Gene expression markers of tumor infiltrating leukocytes. J Immunother Cancer. 2017;5:18.
19. Alexa A, Rahnenfuhrer J. topGO: enrichment analysis for gene ontology. R package version. 2010;2:2010.
20. Mitchell AL, Attwood TK, Babbitt PC, Blum M, Bork P, Bridge A, et al. InterPro in 2019: improving coverage, classification and access to protein sequence annotations. Nucleic Acids Res. 2019;47(D1):D351–60.
21. Geer LY, Marchler-Bauer A, Geer RC, Han L, He J, He S, et al. The NCBI BioSystems database. Nucleic Acids Res. 2010;38(Database issue):D492-6.
22. Subramanian A, Tamayo P, Mootha VK, Mukherjee S, Ebert BL, Gillette MA, et al. Gene set enrichment analysis: a knowledge-based approach for interpreting genome-wide expression profiles. Proc Natl Acad Sci U S A. 2005;102(43):15545–50.
23. Liberzon A, Subramanian A, Pinchback R, Thorvaldsdóttir H, Tamayo P, Mesirov JP. Molecular signatures database (MSigDB) 3.0. Bioinformatics. 2011;27(12):1739–40.
24. Fabregat A, Jupe S, Matthews L, Sidiropoulos K, Gillespie M, Garapati P, et al. The reactome pathway knowledgebase. Nucleic Acids Res. 2018;46(D1):D649–55.
25. Slenter DN, Kutmon M, Hanspers K, Riutta A, Windsor J, Nunes N, et al. WikiPathways: a multifaceted pathway database bridging metabolomics to other omics research. Nucleic Acids Res. 2018;46(D1):D661–7.
26. Malkov VA, Serikawa KA, Balantac N, Watters J, Geiss G, Mashadi-Hossein A, et al. Multiplexed measurements of gene signatures in different analytes using the Nanostring nCounter Assay System. BMC Res Notes. 2009;2:80.
27. Geiss GK, Bumgarner RE, Birditt B, Dahl T, Dowidar N, Dunaway DL, et al. Direct multiplexed measurement of gene expression with color-coded probe pairs. Nat Biotechnol. 2008;26(3):317–25.
28. Han X, Wang W, He J, Jiang L, Li X. Osteopontin as a biomarker for osteosarcoma therapy and prognosis. Oncol Lett. 2019;17(3):2592–8.
29. Lund SA, Giachelli CM, Scatena M. The role of osteopontin in inflammatory processes. J Cell Commun Signal. 2009;3(3–4):311–22.
30. Wai PY, Kuo PC. The role of osteopontin in tumor metastasis. J Surg Res. 2004;121(2):228–41.
31. Zhao J, Dong L, Lu B, Wu G, Xu D, Chen J, et al. Down-regulation of osteopontin suppresses growth and metastasis of hepatocellular carcinoma via induction of apoptosis. Gastroenterology. 2008;135(3):956–68.
32. Mori R, Shaw TJ, Martin P. Molecular mechanisms linking wound inflammation and fibrosis: knockdown of osteopontin leads to rapid repair and reduced scarring. J Exp Med. 2008;205(1):43–51.
33. Ashkar S, Weber GF, Panoutsakopoulou V, Sanchirico ME, Jansson M, Zawaideh S, et al. Eta-1 (osteopontin): an early component of type-1 (cell-mediated) immunity. Science. 2000;287(5454):860–4.
34. Gudowska-Sawczuk M, Mroczko B. What is currently known about the role of CXCL10 in SARS-CoV-2 infection? Int J Mol Sci. 2022;23(7):3673.
35. Huang H, Zhou W, Chen R, Xiang B, Zhou S, Lan L. CXCL10 is a tumor microenvironment and immune infiltration related prognostic biomarker in pancreatic adenocarcinoma. Front Mole Biosci. 2021;8:8.
36. Ariyarathna H, Thomson N, Aberdein D, Munday JS. Chemokine gene expression influences metastasis and survival time of female dogs with mammary carcinoma. Vet Immunol Immunopathol. 2020;227:110075.
37. Russo E, Santoni A, Bernardini G. Tumor inhibition or tumor promotion? The duplicity of CXCR3 in cancer. J Leukoc Biol. 2020;108(2):673–85.

38. Bianchi ME, Mezzapelle R. The chemokine receptor CXCR4 in cell proliferation and tissue regeneration. Front Immunol. 2020;11:2109.
39. Cao Y, Hunter ZR, Liu X, Xu L, Yang G, Chen J, et al. The WHIM-like CXCR4(S338X) somatic mutation activates AKT and ERK, and promotes resistance to ibrutinib and other agents used in the treatment of Waldenstrom's Macroglobulinemia. Leukemia. 2015;29(1):169–76.
40. Laverdiere C, Hoang BH, Yang R, Sowers R, Qin J, Meyers PA, et al. Messenger RNA expression levels of CXCR4 correlate with metastatic behavior and outcome in patients with osteosarcoma. Clin Cancer Res. 2005;11(7):2561–7.
41. Wysolmerski JJ, Philbrick WM, Dunbar ME, Lanske B, Kronenberg H, Broadus AE. Rescue of the parathyroid hormone-related protein knockout mouse demonstrates that parathyroid hormone-related protein is essential for mammary gland development. Development. 1998;125(7):1285–94.
42. Philbrick WM, Dreyer BE, Nakchbandi IA, Karaplis AC. Parathyroid hormone-related protein is required for tooth eruption. Proc Natl Acad Sci U S A. 1998;95(20):11846–51.
43. Foley J, Longely BJ, Wysolmerski JJ, Dreyer BE, Broadus AE, Philbrick WM. PTHrP regulates epidermal differentiation in adult mice. J Invest Dermatol. 1998;111(6):1122–8.
44. Yang R, Hoang BH, Kubo T, Kawano H, Chou A, Sowers R, et al. Overexpression of parathyroid hormone Type 1 receptor confers an aggressive phenotype in osteosarcoma. Int J Cancer. 2007;121(5):943–54.
45. Al-Khan AA, Al Balushi NR, Richardson SJ, Danks JA. Roles of parathyroid hormone-related protein (PTHrP) and its receptor (PTHR1) in normal and tumor tissues: focus on their roles in osteosarcoma. Front Vet Sci. 2021;8:637614.
46. Hu C, Wen J, Gong L, Chen X, Wang J, Hu F, et al. Thrombospondin-1 promotes cell migration, invasion and lung metastasis of osteosarcoma through FAK dependent pathway. Oncotarget. 2017;8(44):75881–92.
47. Liu Y, Cai Y, Liu L, Wu Y, Xiong X. Crucial biological functions of CCL7 in cancer. PeerJ. 2018;6:e4928.
48. Ahmed H, AlSadek DM. Galectin-3 as a potential target to prevent cancer metastasis. Clin Med Insights Oncol. 2015;9:113–21.
49. Mainetti LE, Zhe X, Diedrich J, Saliganan AD, Cho WJ, Cher ML, et al. Bone-induced c-kit expression in prostate cancer: a driver of intraosseous tumor growth. Int J Cancer. 2015;136(1):11–20.
50. Scheu S, Ali S, Ruland C, Arolt V, Alferink J. The C-C Chemokines CCL17 and CCL22 and their receptor CCR4 in CNS autoimmunity. Int J Mol Sci. 2017;18(11):2306.
51. Rauniyar K, Jha SK, Jeltsch M. Biology of vascular endothelial growth factor C in the morphogenesis of lymphatic vessels. Front Bioeng Biotechnol. 2018;6:7.
52. Liu W, Hu H, Shao Z, Lv X, Zhang Z, Deng X, et al. Characterizing the tumor microenvironment at the single-cell level reveals a novel immune evasion mechanism in osteosarcoma. Bone Res. 2023;11(1):4.
53. Park HR, Min K, Kim HS, Jung WW, Park YK. Expression of vascular endothelial growth factor-C and its receptor in osteosarcomas. Pathol Res Pract. 2008;204(8):575–82.
54. Yang W-H, Chang A-C, Wang S-W, Wang S-J, Chang Y-S, Chang T-M, et al. Leptin promotes VEGF-C production and induces lymphangiogenesis by suppressing miR-27b in human chondrosarcoma cells. Sci Rep. 2016;6(1):28647.
55. Wang Z-Q, Liang J, Schellander K, Wagner EF, Grigoriadis AE. c-fos-induced osteosarcoma formation in transgenic mice: cooperativity with c-jun and the role of endogenous c-fos1. Can Res. 1995;55(24):6244–51.
56. Sasaki K, Takano S, Tomizawa S, Miyahara Y, Furukawa K, Takayashiki T, et al. C4b-binding protein α-chain enhances antitumor immunity by facilitating the accumulation of tumor-infiltrating lymphocytes in the tumor microenvironment in pancreatic cancer. J Exp Clin Cancer Res. 2021;40(1):212.
57. Liu K, He Q, Liao G, Han J. Identification of critical genes and gene interaction networks that mediate osteosarcoma metastasis to the lungs. Exp Ther Med. 2015;10(5):1796–806.
58. Criado García O, Sánchez-Corral P, Rodríguez de Córdoba S. Isoforms of human C4b-binding protein. II. Differential modulation of the C4BPA and C4BPB genes by acute phase cytokines. J Immunol. 1995;155(8):4037–43.
59. García de Frutos P, Alim RI, Härdig Y, Zöller B, Dahlbäck B. Differential regulation of alpha and beta chains of C4b-binding protein during acute-phase response resulting in stable plasma levels of free anticoagulant protein S. Blood. 1994;84(3):815–22.
60. Agostinis C, Zorzet S, Balduit A, Zito G, Mangogna A, Macor P, et al. The inflammatory feed-forward loop triggered by the complement component C3 as a potential target in endometriosis. Front Immunol. 2021;12:693118.
61. Pisarcik D, Kousourou G, Vinod N. A case of paraneoplastic arthralgias. Am J Med Case Rep. 2021;9(8):397–401.
62. Matsubara T, Soh J, Morita M, Uwabo T, Tomida S, Fujiwara T, et al. DV200 index for assessing RNA integrity in next-generation sequencing. Biomed Res Int. 2020;2020:9349132.
63. Penland SK, Keku TO, Torrice C, He X, Krishnamurthy J, Hoadley KA, et al. RNA expression analysis of formalin-fixed paraffin-embedded tumors. Lab Invest. 2007;87(4):383–91.
64. Fujii T, Uchiyama T, Matsuoka M, Myojin T, Sugimoto S, Nitta Y, Okabe F, Sugimoto A, Sekita-Hatakeyama Y, Morita K, Itami H, Hatakeyama K, Ohbayashi C. Evaluation of DNA and RNA quality from archival formalin-fixed paraffin-embedded tissue for next-generation sequencing - Retrospective study in Japanese single institution. Pathol Int. 2020;70(9):602–11. https://doi.org/10.1111/pin.12969.

Publisher's Note